Origin, antigenicity, and function of a secreted form of ORF2 in hepatitis E virus infection

Xin Yin[a], Dong Ying[b,c], Sébastien Lhomme[a], Zimin Tang[b], Christopher M. Walker[a,d], Ningshao Xia[b,c], Zizheng Zheng[b,1], and Zongdi Feng[a,d,1]

[a]Center for Vaccines and Immunity, The Research Institute at Nationwide Children's Hospital, Columbus, OH 43205; [b]State Key Laboratory of Molecular Vaccinology and Molecular Diagnostics, National Institute of Diagnostics and Vaccine Development in Infectious Diseases, School of Public Health, Xiamen University, 361102 Xiamen, People's Republic of China; [c]School of Life Science, Xiamen University, 361102 Xiamen, People's Republic of China; and [d]Department of Pediatrics, The Ohio State University College of Medicine, Columbus, OH 43205

Edited by Xiang-Jin Meng, Virginia Polytechnic Institute and State University, Blacksburg, VA, and approved March 23, 2018 (received for review December 8, 2017)

The enterically transmitted hepatitis E virus (HEV) adopts a unique strategy to exit cells by cloaking its capsid (encoded by the viral ORF2 gene) and circulating in the blood as "quasi-enveloped" particles. However, recent evidence suggests that the majority of the ORF2 protein present in the patient serum and supernatants of HEV-infected cell culture exists in a free form and is not associated with virus particles. The origin and biological functions of this secreted form of ORF2 ($ORF2^S$) are unknown. Here we show that production of $ORF2^S$ results from translation initiated at the previously presumed AUG start codon for the capsid protein, whereas translation of the actual capsid protein ($ORF2^C$) is initiated at a previously unrecognized internal AUG codon (15 codons downstream of the first AUG). The addition of 15 amino acids to the N terminus of the capsid protein creates a signal sequence that drives $ORF2^S$ secretion via the secretory pathway. Unlike $ORF2^C$, $ORF2^S$ is glycosylated and exists as a dimer. Nonetheless, $ORF2^S$ exhibits substantial antigenic overlap with the capsid, but the epitopes predicted to bind the putative cell receptor are lost. Consistent with this, $ORF2^S$ does not block HEV cell entry but inhibits antibody-mediated neutralization. These results reveal a previously unrecognized aspect in HEV biology and shed new light on the immune evasion mechanisms and pathogenesis of this virus.

hepatitis E virus | antibody neutralization | immunological decoy | leaky translation | quasi-envelopment

Hepatitis E virus (HEV) is a leading cause of acute hepatitis worldwide (1). Each year HEV infects ~20 million people. At least five HEV genotypes that infect humans are known (2). HEV genotypes 1 and 2 infections occur mostly in developing countries and a high mortality rate in pregnant women infected with genotype 1 HEV has been documented (3). HEV genotypes 3 and 4 are common in developed countries and are mostly transmitted via contaminated meat products (4, 5). Zoonotic transmission of HEV genotype 7 to a human has also recently been described (6). Seroprevalence studies suggest these zoonotic infections are more common than previously appreciated (7). Persistent infections with HEV genotype 3 in immunocompromised individuals can result in rapid progression to fibrosis and cirrhosis (8, 9). Infectious HEV has also been found in the blood supply, raising the possibility of transfusion-mediated transmission (10). To date, HEV is not routinely screened in the clinic due to the low rates of diagnosed acute HEV, as well as the lack of concordance between commercial assays (11–13).

HEV is a single-stranded, positive sense RNA virus belonging to the *Hepeviridae* family. All variants of HEV known to infect humans belong to the species *Orthohepevirus A* (2). The ~7.2-kb HEV genome contains three ORFs. ORF1 is a polyprotein required for HEV RNA replication. ORF2 is the capsid protein, while ORF3 is a small protein involved in HEV egress (14). HEV has a unique dual life cycle: it is shed into the feces as naked virions, but circulates in the blood as "quasi-enveloped" particles (eHEV) (15). Unlike classic enveloped viruses, eHEV particles lack viral antigens on their surface and therefore are insensitive to neutralizing antibodies in standard neutralization assays (16). Intriguingly, recent studies show that large amounts of ORF2 protein are released from HEV-infected cell cultures and also can be detected in the serum of HEV-infected patients (17, 18). The origin and biological significance of the secreted form of ORF2 remain unclear.

In the present study, we show that the secreted form of ORF2 ($ORF2^S$) and the capsid-associated ORF2 ($ORF2^C$) are two different translation products of the viral ORF2 gene. We provide evidence that while $ORF2^S$ is not essential for infection, it may have a role in modulating host antibody responses.

Results

HEV-Infected Cells Release a Large Amount of Nonvirion-Associated ORF2 both in Vitro and in Vivo. Previous studies have demonstrated that HEV is released from infected cells as quasi-enveloped particles (eHEV), and the capsid is hidden within a host membrane and cannot be recognized by anticapsid antibodies unless treated with detergent (11). However, using a commercial HEV antigen ELISA, we detected a high level of the ORF2 protein in the supernatant of HEV-infected cell cultures irrespective of detergent treatment (Fig. 1*A*). Rate-zonal ultracentrifugation revealed that the majority of the ORF2 protein in the culture supernatants was not associated with infectious virions (Fig. 1*B*). Comparison of the protein abundance of ORF2 and ORF3 in the culture supernatant and those in purified eHEV particles

Significance

Hepatitis E virus (HEV) is a main cause of acute hepatitis worldwide. Recent evidence suggests that HEV-infected cells release a secreted form of ORF2 protein ($ORF2^S$) but its origin and function are unknown. Here we demonstrate that $ORF2^S$ and $ORF2^C$ (the actual capsid protein) are different translation products and that $ORF2^S$ is not essential for the HEV life cycle but inhibits antibody-mediated neutralization of HEV. Our results have important implications for understanding the HEV replication cycle and immune evasion mechanisms. The identified internal start codon in this study is highly conserved in most HEV strains, suggesting that the production of $ORF2^S$ is an evolutionary conserved function for HEV.

Author contributions: X.Y., Z.T., Z.Z., and Z.F. designed research; X.Y., D.Y., and S.L. performed research; C.M.W., N.X., and Z.Z. contributed new reagents/analytic tools; X.Y., Z.Z., and Z.F. analyzed data; and X.Y., Z.Z., and Z.F. wrote the paper.

The authors declare no conflict of interest.

This article is a PNAS Direct Submission.

[1]To whom correspondence may be addressed. Email: zhengzizheng@xmu.edu.cn or Zongdi.Feng@nationwidechildrens.org.

This article contains supporting information online at www.pnas.org/lookup/suppl/doi:10.1073/pnas.1721345115/-/DCSupplemental.

Published online April 18, 2018.

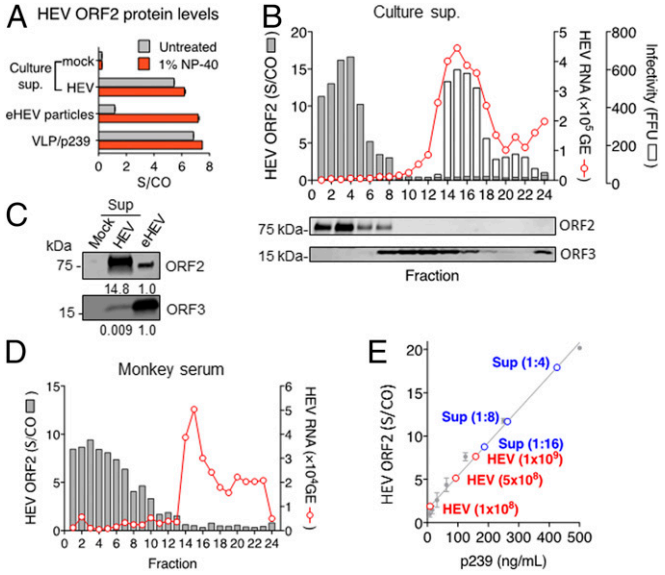

Fig. 1. HEV-infected cells release a large amount of nonvirion-associated ORF2 protein both in vitro and in vivo. (*A*) Detection of HEV ORF2 protein in culture supernatants (sup) (1:32 dilution) of mock or HEV (Kernow C1/p6) persistently infected Huh-7 cells, purified quasi-enveloped HEV particles (eHEV) (10^9 GE), and HEV VLP p239 (12.5 ng) with or without 1% Nonidet P-40 treatment. HEV ORF2 protein was measured by a commercial HEV antigen ELISA (Wantai). Signal to cut-off (S/CO) ratio was determined based on optical density values measured at 450 nm. Data represent mean ± SEM from two independent experiments each in duplicate wells. (*B*, *Upper*) Rate-zonal gradient profile of HEV RNA, ORF2 protein, and infectious virions in the culture supernatant of HEV-infected Huh-7 cells. Fractions were collected from the top of the gradient. (*Lower*) Western blots of HEV ORF2 and ORF3 in the same gradient fractions (each lane contained two consecutive fractions) with a chimpanzee convalescent serum (Ch1313) and a rabbit anti-ORF3 antibody, respectively. (*C*) Protein abundance of HEV ORF2 and ORF3 in culture supernatants of HEV persistently infected Huh-7 cells and gradient purified eHEV particles (~10^9 GE). The relative protein abundance is shown below each blot. (*D*) Rate-zonal gradient profile of HEV RNA and ORF2 protein in a serum sample from a genotype 3 HEV (Kernow C1)-infected rhesus macaque. (*E*) ELISA quantitation of HEV ORF2 protein in the culture supernatant with different dilutions and Nonidet P-40-treated purified eHEV particles. Serially diluted VLP (p239) was used for creating a standard curve.

indicated that less than 0.1% (0.009/14.8 × 100%) of the total ORF2 protein in the supernatants was associated with virions (Fig. 1*C*). Similarly, the majority of ORF2 protein present in the serum of an HEV-infected macaque was not virion-associated (Fig. 1*D*). Using HEV virus-like particles (VLP) p239 as an ELISA standard, we estimated that the concentration of the ORF2 protein in HEV persistently infected culture supernatants was ~1.5–3 μg/mL, whereas 10^9 highly concentrated virions contained ~0.2 μg ORF2 (Fig. 1*E*). The detection limit of the commercial HEV antigen ELISA for virions was estimated to be 6.2×10^7 particles [based on HEV genome equivalents (GE)]. Because HEV RNA titers in culture supernatants and patient serum samples rarely exceed 10^7 GE/mL (11, 19), the secreted form of ORF2 is likely the exclusive target of the commercial antigen ELISA. In the following experiments, we used the term ORF2^S for the secreted, nonvirion-associated ORF2, and ORF2^C for the actual capsid protein.

ORF2^S Exists as a Glycosylated Dimer. The protein size of ORF2^S was larger than ORF2^C (84 kDa vs. 72 kDa) (Fig. 1*C*), suggesting that ORF2^S is posttranslationally modified. It has been shown that ORF2 becomes glycosylated when overexpressed (20). Consistent with this, treatment of ORF2^S with either PNGase-F, which removes the *N*-linked glycans from proteins, or O-glycosidase and neuraminidase, which remove O-linked glycans, reduced the size of ORF2^S (Fig. 2*A*) [ORF2^S (WT)]. The three putative *N*-linked glycosylation sites described in previous studies likely contributed to the glycosylation of ORF2^S (Fig. 2*A*) [ORF2^S (N137/310/562Q)]. In contrast, the size of ORF2^C was not reduced by these treatments (Fig. 2*A*, virions). Moreover, treatment of HEV-infected cells with brefeldin A, an inhibitor of protein transport from the endoplasmic reticulum (ER) to the Golgi apparatus, resulted in intracellular accumulation of slower-migrating ORF2 proteins, along with a dramatic reduction of ORF2^S in the culture supernatant (Fig. 2*B*). These results demonstrated that ORF2^S is released through the classic secretory pathway and its release is rather efficient.

ORF2^S sedimented more slowly in a rate-zonal gradient than HEV VLP p239, which consists of 60 copies of a truncated ORF2 protein comprising amino acids 368–606 (21) (Fig. S1). This suggested that ORF2^S does not exist in a high-order particulate form. In addition to the major 84-kDa species, we routinely detected a minor ~170-kDa species, suggesting that ORF2^S forms a dimer (Fig. 2*C*). Unboiled ORF2^S migrated predominantly as an ~170-kDa species, indicating that the majority of ORF2^S exists in a dimeric form. The ratio of ORF2^S dimers and monomers did not change under a nonreducing condition (Fig. 2*C*), indicating that ORF2^S dimerization does not require disulfide bonds, a property that is shared with ORF2^C (22).

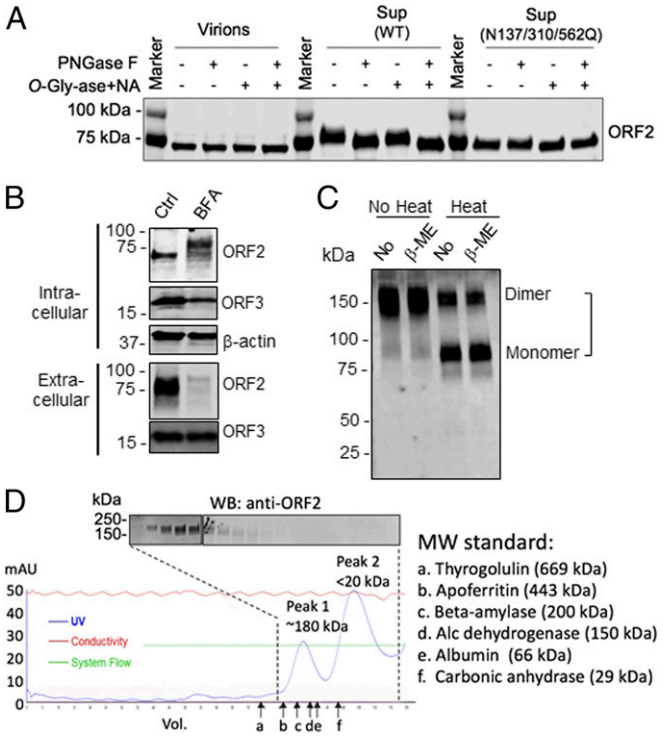

Fig. 2. The secreted form of ORF2 (ORF2^S) is glycosylated and dimerized. (*A*) Effects of PNGase F, O-glycosidase (O-Gly-ase), and neuraminidase (NA) treatment on ORF2 in virions and in supernatants of Huh-7 cells transfected with a WT HEV RNA or a variant carrying mutations in three putative *N*-linked glycosylation sites (N137/310/562Q). ORF2 was detected by a chimpanzee convalescent serum (Ch1313). (*B*) HEV persistently infected Huh-7 cells were treated with brefeldin A (BFA) for 24 h or left untreated (Ctrl). Cells and supernatants were collected and analyzed by immunoblotting with indicated antibodies. (*C*) Effects of β-mecaptomethanol (β-ME) and heat treatment (95 °C, 10 min) on the size of ORF2^S in a native protein gel. (*D*) Determination of the size of ORF2^S by size-exclusion chromatography. The majority of ORF2^S was eluted as peak 1 with an estimated size of 180 kDa. The column contaminants were eluted in the second peak (peak 2). The presence of ORF2^S in peak fractions was confirmed by Western blot analysis using Ch1313.

The dimeric nature of ORF2^S was further confirmed by size-exclusion chromatography (Fig. 2*D*).

ORF2^S and ORF2^C Are Different Translation Products of the ORF2 Gene. The difference in the size and glycosylation pattern between ORF2^S and ORF2^C suggested that either they are the same proteins subjected to differential posttranslational regulations, or they are different translation products of the ORF2 gene. Sequence alignment revealed a highly conserved internal AUG codon located at 15 codons downstream of the presumed AUG start codon for the capsid (Table S1). We reasoned that both AUGs might be active in infected cells. Because the N terminus of the presumed full-length ORF2 protein contains a putative signal peptide (amino acids 1–23) (www.cbs.dtu.dk/services/SignalP), translation from the first AUG would produce a full-length protein with a signal peptide that could direct the protein into the secretory pathway (i.e., ORF2^S), whereas translation from the internal AUG codon would disrupt the signal sequence, producing a cytoplasmic protein that is responsible for virion assembly (i.e., ORF2^C) (Fig. 3*A*). To test this hypothesis, we generated mutant HEV RNAs in which the two AUG codons were inactivated, either alone (mut1 and mut2) or in combination (mut1+2). All mutants replicated at comparable levels to the WT HEV, as evidenced by the similar intracellular HEV RNA levels 5 d after RNA transfection (Fig. 3*B*). We then determined the levels of intracellular and extracellular ORF2 by indirect immunofluorescence assay (IFA) and Western blot analysis (Fig. 3 *C* and *D*). Mutation of the first AUG codon resulted in a substantial decrease of intracellular ORF2 expression and a complete loss of ORF2^S in the culture supernatant (Fig. 3 *C* and *D*, mut1). In contrast, mutation of the internal AUG codon resulted in no changes in either the intracellular or the extracellular ORF2 levels (Fig. 3 *C* and *D*, mut2). Mutation of both AUG codons resulted in a complete loss of both intracellular and extracellular ORF2 expression (Fig. 3 *C* and *D*, mut1+2). Importantly, infectious virions were produced in cells transfected with WT or mut1 HEV RNA, but not in cells transfected with mut2 or mut1+2 RNA (Fig. 3 *E*–*G*). Similar results were obtained with a genotype 1 HEV strain (Fig. S2). Collectively, these results demonstrated that the first AUG codon, which has long been believed to be the initiation codon for the HEV capsid protein, is indeed responsible for the translation of the secreted form of ORF2 (ORF2^S), whereas the highly conserved internal AUG codon encoding methionine (Met) 16 is responsible for translation of the capsid protein ORF2^C.

To corroborate the above results, we adopted a trans-complementation system developed by Ding et al. (23). In this system, ORF2 and ORF3 are provided *in trans* by lentivirus vectors, and transfection of a replication-competent HEV subgenomic RNA into cells expressing ORF2 and ORF3 results in infectious virus particle assembly and release. We created cell

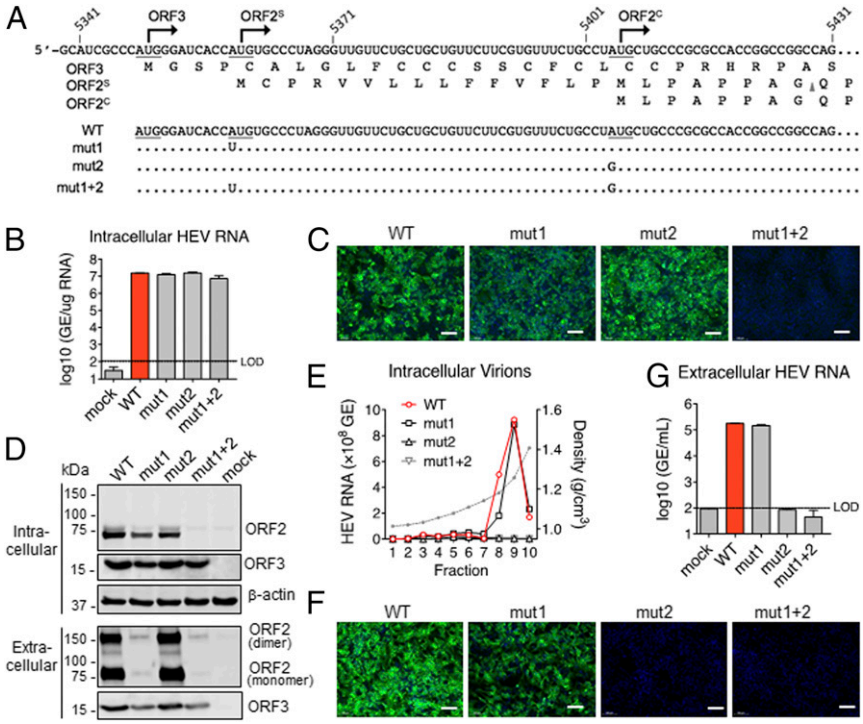

Fig. 3. ORF2^S and ORF2^C are different translation products of the HEV ORF2 gene. (*A*) The N terminus sequence of the HEV subgenomic RNA (Kernow C1/p6) and strategies for site-directed mutagenesis. The AUG start codons for ORF3, ORF2^S, and ORF2^C are underlined, and the corresponding protein sequences are shown below. The first AUG and the internal AUG codons of the ORF2 gene are mutated either singly (mut1 and mut2) or in combination (mut1+2) without altering the amino acid sequence of ORF3. The putative signal peptide cleavage site in ORF2^S is indicated (arrowhead). (*B*) qRT-PCR analysis of intracellular RNA levels in Huh-7 cells transfected with in vitro transcripts of WT or mutant HEV RNA (5-d posttransfection). Data are shown as mean ± SEM of two independent experiments each performed in duplicate wells. LOD, limit of detection. (*C*) Huh-7 cells transfected with WT or mutant HEV RNA for 5 d were stained with a chimpanzee convalescent serum Ch1313 (green). Nuclei were stained with DAPI (blue). (Scale bars, 100 μm.) (*D*) Immunoblots of intracellular and extracellular ORF2 and ORF3 proteins at 5 d after HEV RNA transfection into Huh-7 cells. β-Actin was used as a loading control. ORF2 was detected by Ch1313. ORF3 was detected with a rabbit anti-ORF3 antibody. (*E*) Isopycnic gradient profile of intracellular HEV RNA (as a surrogate marker of virions) in Huh-7 cells transfected with different HEV RNA (15-d posttransfection). Cells were freeze-thawed three times and treated with RNase before gradient centrifugation. Fractions were collected from the top of the gradient. (*F* and *G*) HepG2/shMAVS cells were inoculated with equal amounts of WT or mutant HEV (10,000 GE per cell) isolated from HEV RNA-transfected Huh-7 cells. Cells were stained with Ch1313 (green) and DAPI (blue) at 5-d postinoculation (*F*). (Scale bars, 100 μm.) Supernatant HEV RNA levels (5 d after inoculation) were measured by qRT-PCR (*G*). Data are shown as mean ± SEM of two independent experiments each performed in duplicate wells.

lines that stably express ORF3 along with different ORF2 variants (WT, mut1, and mut2), followed by transfection with a GFP-expressing HEV replicon RNA that lacks both ORF2 and ORF3. We found that cells expressing WT or mut1 ORF2 produced comparable amounts of infectious virions, but cells expressing mut2 produced none (Fig. S3). These results again demonstrated that the internal AUG codon is responsible for initiating the translation of the capsid protein.

Montpellier et al. (18) recently reported that the N-terminal sequence of the ORF2 in purified HEV virions begins at leucine (Leu) 14, instead of Met16. However, cells expressing ORF2 that contains amino acids 14–660 barely produced any infectious particles (Fig. S3). The low level of infectious virions produced from these cells was likely due to leaky translation of $ORF2^C$ from Met16, as inactivation of this internal AUG codon led to a further reduction in infectious virus production. Mass spectrometry (MS) analyses of highly purified HEV virions identified Leu17 as the N-terminal residue of $ORF2^C$ (Fig. S4), providing further evidence that $ORF2^C$ is translated from the internal AUG start codon.

Interestingly, the ORF2 protein level in mut1 RNA-transfected cells was much less than in cells transfected with WT or mut2 RNA. This result indicates that most intracellular ORF2 is derived from $ORF2^S$. In agreement with this, a *Gaussia* luciferase placed behind the AUG codon for $ORF2^S$ was more efficiently translated (~fivefold) than that placed behind the AUG codon for $ORF2^C$ (Fig. S5). Confocal microscopy indicated that neither the intracellular $ORF2^S$ nor $ORF2^C$ was associated with the ER or the Golgi apparatus (Fig. S6), suggesting that the intracellular $ORF2^S$ predominantly resides in the cytoplasm. To better understand how $ORF2^S$ accumulated in the cytoplasm, we determined the N-terminal and C-terminal sequences of both extracellular and intracellular $ORF2^S$ by MS. The result indicated that the extracellular $ORF2^S$ included amino acids 34–660, consistent with a recent report (18), while the intracellular $ORF2^S$ included amino acids 12–660 (Fig. S4). The absence of the first 11 amino acids would disrupt the transmembrane domain of the signal sequence, providing a plausible explanation for the observation that some $ORF2^S$ was retained in infected cells.

$ORF2^S$ Is Antigenically Similar but Not Identical to $ORF2^C$ in Virions. Because the commercial HEV antigen ELISA detects $ORF2^S$, VLP, and virions (Fig. 1*A*), we sought to compare their antigenicity using a panel of conformation-dependent monoclonal antibodies (mAbs) that recognize six different antigenic clusters (C1–C6) on the HEV capsid (24) (Fig. 4*A*). As some of these mAbs were generated using genotype 1 ORF2, we included different genotypes for comparison. A recombinant ORF2 dimer (rDimer) comprising amino acids 394–606 was also included (21). mAbs 12F12 and #4, which are used in the commercial HEV antigen ELISA (25), recognized all four forms of ORF2 (rVLP, rDimer, $ORF2^S$, and virions) of all genotypes tested (g1, g3, and g4), therefore were used to adjust the input amounts of different ORF2 forms.

This analysis revealed substantial antigenic overlap between $ORF2^S$ and other forms of ORF2-including virions (Fig. 4*B*). The most noticeable difference was the loss of the C3 and C4 epitopes on $ORF2^S$ for genotype 3 HEV. These epitopes are located at the top region of the protrusion (P) domain of the capsid and have been implicated for receptor binding (26).

It is worth noting that mAbs specific to the C5 and C6 epitopes, which are located in the "groove zone" of ORF2 in the crystal structure, possess potent neutralizing activity (24). This suggests that major neutralizing epitopes are preserved in $ORF2^S$. Unexpectedly, the C2 epitope, which is recognized by a pan-genotypic mAb 8G12 (27), appeared to be lost in the Kernow strain that we used in this study. The loss of this epitope is likely due to an amino acid change at position 554 (K554 → R), because K554 constitutes a key residue for the C2 epitope and is highly conserved in human HEV strains (27). Indeed, changing R554 to the conserved residue K reinstated the C2 epitope on both $ORF2^S$ and virions (Fig. 4*B*, p6 554K). Interestingly, this mutation also reinstated the C3 epitope on virions, possibly due to a change in the local conformation as an adjacent residue T553 is important for the C3 epitope (24). However, the C3 epitope remained lost on $ORF2^S$ in the 554K mutant.

$ORF2^S$ Does Not Block HEV Entry, but Impairs Antibody-Mediated Neutralization. Because $ORF2^S$ antigenically overlapped with virions and was released in great excess to virions, we investigated if $ORF2^S$ inhibits HEV entry by competition for the cell

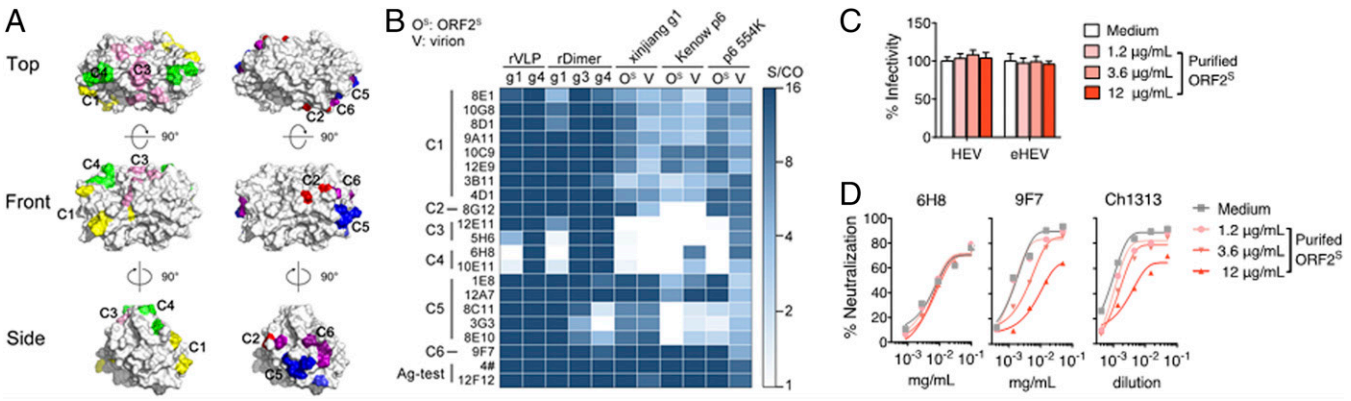

Fig. 4. $ORF2^S$ antigenically overlaps with virions and interferes with antibody-mediated neutralization but not entry of HEV. (*A*) Location of six distinct antigenic clusters (C1–C6) on the protrusion domain of the HEV capsid (genotype 1). (*B*) Comparison of antigenicity of HEV recombinant VLP (rVLP, genotypes 1 and 4), recombinant ORF2 dimer (rDimer, genotypes 1, 3, and 4), $ORF2^S$ (O^S), and virions (V) [Xinjiang-1 (genotype 1), Kernow C1/p6 (genotype 3)] in a sandwich ELISA with a rabbit anti-ORF2 antibody as a capture antibody and indicated anti-ORF2 monoclonal antibodies as the detection antibody. (*C*) Nonenveloped HEV or eHEV particles (1,000 GE per cell) were incubated with indicated concentrations of purified $ORF2^S$ (37 °C, 1 h) before inoculation of HepG2/shMAVS cells. Relative infectivity was calculated based on the numbers of foci determined by indirect IFAs with Ch1313 5 d later. Data represent mean ± SEM of two independent experiments each performed in duplicate wells. (*D*) Serially diluted monoclonal (6H8 and 9F7) or polyclonal (Ch1313) anti-HEV antibodies were mixed with indicated concentrations of purified $ORF2^S$ at 37 °C for 2 h before incubation with HEV (1×10^7 GE) for another 2 h. The mixture was then inoculated to HepG2 cells (4×10^4 cells per well). Percent neutralization was calculated based on the number of HEV^+ foci 5 d after inoculation. Shown are representative results from two independent experiments.

receptors. This appeared not to be the case, as preincubation of either nonenveloped HEV or eHEV particles with high concentrations of purified $ORF2^S$ had no impact on virus infectivity (Fig. 4*C*). Consistent with this, cell binding of $ORF2^S$ was much less efficient than VLPs (Fig. S7*A*).

We next determined the effect of $ORF2^S$ on antibody-mediated neutralization of HEV. Purified $ORF2^S$ dose-dependently inhibited the neutralizing activity of mAb 9F7, a potent neutralizing antibody recognizing the C6 epitope (24) (Fig. 4*D*). However, under the same condition, no inhibition was observed for mAb 6H8, which recognizes the C4 epitope. These results are consistent with the presence of the C6 epitope and absence of the C4 epitope on $ORF2^S$. To investigate if $ORF2^S$ also affects neutralization by antibodies generated by infection, we used a hyperimmune plasma from a chimpanzee infected with HEV (Ch1313) (28). A dose-dependent inhibition by $ORF2^S$ was also observed. The inhibitory effect of $ORF2^S$ on antibody-mediated neutralization of HEV was also confirmed with a VLP cell-binding assay (Fig. S7*B*).

Discussion

The presence of large amounts of nonvirion-associated ORF2 protein in HEV-infected cell culture supernatants and patient sera remains puzzling. In this study, we identified the origin of this secreted form of ORF2, which we termed $ORF2^S$, and investigated its function in a cell-culture system. We demonstrated that $ORF2^S$ is a different translation product from $ORF2^C$, the actual capsid protein, whose translation is initiated at a previously unrecognized internal AUG codon. The difference in the N-terminal sequences of $ORF2^S$ and $ORF2^C$ results in different fates: most $ORF2^S$ is secreted into the extracellular space as a glycosylated dimer, whereas $ORF2^C$ remains in the cytosol and assembles into infectious virus particles. Our analyses using a panel of conformation-dependent mAbs revealed substantial antigenic overlap between $ORF2^S$ and virions and the major neutralizing epitopes are preserved in $ORF2^S$. However, $ORF2^S$ has a selective loss of epitopes involved in cell binding. Consistent with this, $ORF2^S$ inhibited antibody-mediated neutralization of HEV, but it did not block HEV cell binding and entry. Thus, our study revealed a previously unrecognized aspect in HEV biology, which may have important implications for understanding HEV infection and pathogenesis.

Translation of multiple proteins from the same mRNA is not uncommon for viruses as a way to increase their coding capacity (29–31). Interestingly, HEV ORF3 also has several in-frame start codons, and the first AUG has long been assumed to be the translation initiation codon for ORF3 (32). However, later work showed that the third AUG (not the first AUG) is the authentic ORF3 initiation codon (33). ORF3 is not required for HEV replication in cell culture (34), but it is absolutely necessary for in vivo (pigs and rhesus monkeys) infectivity (35, 36). Intriguingly, the protein size of ORF3 in HEV-infected liver biopsies appears to be larger than that in infected cell cultures (37), raising the possibility that additional protein forms may exist for ORF3 in vivo.

Our findings provide an explanation for the multiple ORF2 forms described in the literature (20, 38). In a recent study, Montpellier et al. (18) reported that HEV-infected PLC/PRL/5 human hepatoma cells also secrete abundant ORF2 protein. The major species, termed "ORF2g" in their study, was also found to be glycosylated and has a similar molecular weight to $ORF2^S$ in our study. Interestingly, they also detected a minor truncated form of ORF2, termed "ORF2c," which lacks the N-terminal 233 amino acids. This truncated form of ORF2 was also detected in some, but not all, of the serum samples from HEV-infected patients (18). We did not detect this truncated form in our system even with the same antibody that was used in the Montpellier study (Fig. S8). Further work will be needed to clarify this issue.

The substantial antigenic overlap between $ORF2^S$ and HEV virions explains the detection of serum antigen by the commercial antigen ELISA. $ORF2^S$ is recognized by mAbs that recognize the C1, C2, C5, and C6 epitopes, among which C2, C5 and C6 are neutralizing epitopes. This is consistent with the observation that $ORF2^S$ inhibited antibody-mediated neutralization. However, the C3 and C4 epitopes located at the top region of the protrusion domain appeared to be lost in $ORF2^S$. Because the top region is implicated for receptor binding, loss of these epitopes likely accounts for the lack of inhibition of HEV entry by $ORF2^S$. It is possible that the *N*-linked glycosylation at N562, which is a key residue in the C3 epitope (24), may mask these epitopes. Alternatively, $ORF2^S$ may assume a different conformation from the dimer formed by $ORF2^C$. It may be worthwhile to determine the structure of $ORF2^S$ in the future to better understand the commonalities and differences between $ORF2^S$ and $ORF2^C$. Several amino acids (Y557, T564, V598, A599, L601) have been identified to be essential for $ORF2^C$ dimerization (22). Thus, it will be interesting to examine if these amino acids are also involved in $ORF2^S$ dimerization.

The role of $ORF2^S$ in natural HEV infection remains to be investigated. Our data indicate that $ORF2^S$ is not essential for the HEV life cycle in cultured cells, but it is able to reduce antibody-mediated neutralization. Therefore, $ORF2^S$ may act as a decoy against the humoral immunity during HEV infection, which is noteworthy, as the eHEV particles that circulate in the bloodstream are insensitive to neutralizing antibodies in standard neutralization assays (16). It is important to note that our previous work demonstrates that while neutralizing anticapsid antibodies do not bind and neutralize free quasi-enveloped hepatitis A virus (eHAV) particles, they can reduce eHAV infectivity via a postentry mechanism (39). A similar mechanism may be at work during HEV infection. Thus, $ORF2^S$ may serve as an additional mechanism for antibody evasion. It is certainly possible that $ORF2^S$ plays additional immunomodulatory roles in natural HEV infection. Given the serum HEV antigen levels are higher in chronic hepatitis E patients (11), $ORF2^S$ could have more dramatic immunomodulatory effects during HEV persistence. Future studies using animal models (e.g., macaques) are warranted to elucidate the functions of $ORF2^S$ in natural HEV infection.

It is also important to recognize that HEV is found in a wide range of animal species (5, 40). While our work is exclusively focused on *Othohepevirus* A including genotypes 1, 3, and 4, an alignment of *Orthohepevirus* B, *Orthohepevirus* C1, moose HEV, and little egret HEV suggests that these viruses may employ a similar strategy, but *Orthohepevirus* C2 and kestrel HEV do not appear to follow this strategy (Table S1). Studies of the roles of different forms of ORF2 may provide unique insights into the evolution of HEV.

In summary, we have identified the secreted form of ORF2 as a different translation product from the HEV capsid protein and demonstrated its ability to reduce antibody-mediated neutralization of HEV. Further characterization of the structure and function of $ORF2^S$ will likely lead to a better understanding of HEV infection and immunity.

Materials and Methods

Cells and Viruses. Huh-7 cells (S10-3 clone) were obtained from Suzanne Emerson, National Institute of Allergy and Infectious Diseases, NIH, Bethesda, MD. HepG2 (C3A clone) cells were purchased from ATCC (CRL-10741). PLC/PRF5 cells were kindly provided by Mark Peeples, Nationwide Children's Hospital, Columbus, OH. Cells were propagated in DMEM containing 10% FBS, 100 U/mL penicillin and 100 μg/mL streptomycin. HepG2 cells transduced with lentivirus expressing shRNA targeting MAVS (shMAVS) were described previously (41). HEV infectious clones of the Kernow-C1 (genotype 3) and the Sar55 (genotype 1) strains were kindly provided by Suzanne Emerson, National Institute of Allergy and Infectious Diseases, NIH, Bethesda, MD. The Xinjiang-1 (genotype 1, DDBJ accession no. D11092) strain was isolated from

stool specimens of hepatitis E patients during an outbreak in Xinjiang (42). HEV stocks were generated by transfecting S10-3 cells with in vitro transcribed HEV genomic RNA.

Plasmids. The infectious cDNA clones of the HEV Sar55 and Kernow C1/p6 strains were used as templates for mutagenesis using a QuikChange II XL site-directed mutagenesis kit (Agilent Technologies). All PCR derived fragments were sequenced to ensure no unwanted mutations were introduced. HEV p6/EGFP was generated using fusion PCR to replace the ORF2 fragment with the *egfp* gene, as described previously (33). For ORF2 overexpression, lentiviral constructs containing Kernow C1/p6 ORF2 and ORF3 (a gift from Alexander Ploss, Princeton University, Princeton, NJ) were used. All of the constructs were validated by sequencing. Primer sequences are provided in Table S2.

Virus Infection and Neutralization. One day before infection, HepG2 cells (2×10^4) were seeded onto 96-well plates coated with rat tail collagen type 1 (Millipore). Cells were inoculated with purified HEV in the presence or absence of ORF2^S for 6 h at 34.5 °C. After washing three times with PBS, cells were refed with DMEM supplemented with 10% FBS and 2% dimethyl sulfoxide (DMSO) and cultured at 34.5 °C. For neutralization assays, antibodies were first incubated with purified ORF2^S for 1 h at 37 °C and subsequently mixed with virus and further incubated at 37 °C for 1 h before inoculation of the HepG2 cells. Cells were stained with an antibody against ORF2 [chimpanzee immune serum (Ch1313) or monoclonal antibody #4] 5 d after inoculation. The extent of neutralization was determined by the number of infected cells in each condition.

Quantification of HEV RNA and Antigen. HEV RNA levels were quantified by real-time quantitative (qRT)-PCR (43). A synthetic full-length HEV Kernow C1/p6 or Sar55 RNA served as standards. HEV ORF2 (capsid) antigen in the culture supernatants and monkey sera was detected by a commercial ELISA (Beijing Wantai Biological Pharmacy Enterprise Co.) and quantified using HEV-like particles (VLPs) p239 as standards (21). An in-house sandwich ELISA was used to compare the antigenicity of ORF2^S, HEV virions, and VLPs, using a rabbit anti-ORF2 antibody as the capture antibody and different conformation-dependent monoclonal antibodies as the detection antibody (24). Detailed procedures are provided in *SI Materials and Methods*.

Statistical Analysis. Statistical analyses were performed using GraphPad Prism (GraphPad). Unpaired Student *t* tests were used to obtain *P* values between groups.

ACKNOWLEDGMENTS. We thank Suzanne Emerson and Patricia Farci (National Institute of Allergy and Infectious Diseases) for providing the hepatitis E virus infectious clones and chimpanzee convalescent serum; Alexander Ploss (Princeton University) for providing the lentiviral constructs containing ORF2 and ORF3; Charuta Ambardekar, Zhimin Hu, Liwen Zhang, and Supranee Chaiwatpongsakorn for technical assistance; Haitao Guo (Indiana University) for helpful discussions; and Mark Peeples (Nationwide Children's Hospital) for critical reading of the manuscript. This work is supported by the National Natural Science Foundation of China Grant 81701576 (to Z.T.); Natural Science Foundation of Fujian Province, China Grant 2016J05201; Principal Funds from Xiamen University (to Z.Z.); the Pinnacle Research Award in Liver Diseases from the American Association for the Study of Liver Diseases Foundation; National Institute of Allergy and Infectious Diseases Grants AI122228 and AI137912; and internal start-up funds from the Nationwide Children's Hospital (to Z.F.). The fusion Orbitrap instrument is supported by an NIH Grant (S10 OD018056) awarded to the Ohio State University Campus Chemical Instrument Center.

1. Kamar N, et al. (2017) Hepatitis E virus infection. *Nat Rev Dis Primers* 3:17086.
2. Smith DB, et al.; International Committee on Taxonomy of Viruses Hepeviridae Study Group (2014) Consensus proposals for classification of the family Hepeviridae. *J Gen Virol* 95:2223–2232.
3. Pérez-Gracia MT, Suay-García B, Mateos-Lindemann ML (2017) Hepatitis E and pregnancy: Current state. *Rev Med Virol* 27:e1929.
4. Meng XJ (2013) Zoonotic and foodborne transmission of hepatitis E virus. *Semin Liver Dis* 33:41–49.
5. Pavio N, Meng XJ, Doceul V (2015) Zoonotic origin of hepatitis E. *Curr Opin Virol* 10:34–41.
6. Lee GH, et al. (2016) Chronic infection with camelid hepatitis E virus in a liver transplant recipient who regularly consumes camel meat and milk. *Gastroenterology* 150: 355–357.e3.
7. Kuniholm MH, Engle RE, Purcell RH, Nelson KE (2015) Hepatitis E virus seroprevalence in the United States: No easy answers. *Hepatology* 61:1441–1442.
8. Dalton HR, Bendall RP, Keane FE, Tedder RS, Ijaz S (2009) Persistent carriage of hepatitis E virus in patients with HIV infection. *N Engl J Med* 361:1025–1027.
9. Kamar N, et al. (2008) Hepatitis E virus and chronic hepatitis in organ-transplant recipients. *N Engl J Med* 358:811–817.
10. Nelson KE (2014) Transmission of hepatitis E virus by transfusion: What is the risk? *Transfusion* 54:8–10.
11. Behrendt P, et al. (2016) Hepatitis E virus (HEV) ORF2 antigen levels differentiate between acute and chronic HEV infection. *J Infect Dis* 214:361–368.
12. Zhao C, et al. (2015) Evaluation of an antigen-capture EIA for the diagnosis of hepatitis E virus infection. *J Viral Hepat* 22:957–963.
13. Bendall R, Ellis V, Ijaz S, Thurairajah P, Dalton HR (2008) Serological response to hepatitis E virus genotype 3 infection: IgG quantitation, avidity, and IgM response. *J Med Virol* 80:95–101.
14. Yin X, Li X, Feng Z (2016) Role of envelopment in the HEV life cycle. *Viruses* 8:229.
15. Feng Z, Hirai-Yuki A, McKnight KL, Lemon SM (2014) Naked viruses that are't always naked: Quasi-enveloped agents of acute hepatitis. *Annu Rev Virol* 1:539–560.
16. Takahashi M, et al. (2010) Hepatitis E virus (HEV) strains in serum samples can replicate efficiently in cultured cells despite the coexistence of HEV antibodies: Characterization of HEV virions in blood circulation. *J Clin Microbiol* 48:1112–1125.
17. Qi Y, et al. (2015) Hepatitis E virus produced from cell culture has a lipid envelope. *PLoS One* 10:e0132503.
18. Montpellier C, et al. (2018) Hepatitis E virus lifecycle and identification of 3 forms of the ORF2 capsid protein. *Gastroenterology* 154:211–223.e8.
19. Lhomme S, et al. (2012) Hepatitis E virus quasispecies and the outcome of acute hepatitis E in solid-organ transplant patients. *J Virol* 86:10006–10014.
20. Zafrullah M, Ozdener MH, Kumar R, Panda SK, Jameel S (1999) Mutational analysis of glycosylation, membrane translocation, and cell surface expression of the hepatitis E virus ORF2 protein. *J Virol* 73:4074–4082.
21. Li SW, et al. (2005) Mutational analysis of essential interactions involved in the assembly of hepatitis E virus capsid. *J Biol Chem* 280:3400–3406.
22. Li S, et al. (2009) Dimerization of hepatitis E virus capsid protein E2s domain is essential for virus-host interaction. *PLoS Pathog* 5:e1000537.
23. Ding Q, et al. (2017) Hepatitis E virus ORF3 is a functional ion channel required for release of infectious particles. *Proc Natl Acad Sci USA* 114:1147–1152.
24. Zhao M, et al. (2015) A comprehensive study of neutralizing antigenic sites on the hepatitis E virus (HEV) capsid by constructing, clustering, and characterizing a tool box. *J Biol Chem* 290:19910–19922.
25. Wen GP, et al. (2015) A valuable antigen detection method for diagnosis of acute hepatitis E. *J Clin Microbiol* 53:782–788.
26. Yamashita T, et al. (2009) Biological and immunological characteristics of hepatitis E virus-like particles based on the crystal structure. *Proc Natl Acad Sci USA* 106: 12986–12991.
27. Gu Y, et al. (2015) Structural basis for the neutralization of hepatitis E virus by a cross-genotype antibody. *Cell Res* 25:604–620.
28. Emerson SU, et al. (2004) In vitro replication of hepatitis E virus (HEV) genomes and of an HEV replicon expressing green fluorescent protein. *J Virol* 78:4838–4846.
29. Chenik M, Chebli K, Blondel D (1995) Translation initiation at alternate in-frame AUG codons in the rabies virus phosphoprotein mRNA is mediated by a ribosomal leaky scanning mechanism. *J Virol* 69:707–712.
30. Kobayashi T, Watanabe M, Kamitani W, Tomonaga K, Ikuta K (2000) Translation initiation of a bicistronic mRNA of Borna disease virus: A 16-kDa phosphoprotein is initiated at an internal start codon. *Virology* 277:296–305.
31. Firth AE, Brierley I (2012) Non-canonical translation in RNA viruses. *J Gen Virol* 93: 1385–1409.
32. Tam AW, et al. (1991) Hepatitis E virus (HEV): Molecular cloning and sequencing of the full-length viral genome. *Virology* 185:120–131.
33. Graff J, Torian U, Nguyen H, Emerson SU (2006) A bicistronic subgenomic mRNA encodes both the ORF2 and ORF3 proteins of hepatitis E virus. *J Virol* 80:5919–5926.
34. Emerson SU, Nguyen H, Torian U, Purcell RH (2006) ORF3 protein of hepatitis E virus is not required for replication, virion assembly, or infection of hepatoma cells in vitro. *J Virol* 80:10457–10464.
35. Graff J, et al. (2005) In vitro and in vivo mutational analysis of the 3′-terminal regions of hepatitis e virus genomes and replicons. *J Virol* 79:1017–1026.
36. Huang YW, Opriessnig T, Halbur PG, Meng XJ (2007) Initiation at the third in-frame AUG codon of open reading frame 3 of the hepatitis E virus is essential for viral infectivity in vivo. *J Virol* 81:3018–3026.
37. Sayed IM, et al. (2017) Study of hepatitis E virus infection of genotype 1 and 3 in mice with humanised liver. *Gut* 66:920–929.
38. Torresi J, Li F, Locarnini SA, Anderson DA (1999) Only the non-glycosylated fraction of hepatitis E virus capsid (open reading frame 2) protein is stable in mammalian cells. *J Gen Virol* 80:1185–1188.
39. Feng Z, et al. (2013) A pathogenic picornavirus acquires an envelope by hijacking cellular membranes. *Nature* 496:367–371.
40. Purdy MA, et al.; Ictv Report Consortium (2017) ICTV virus taxonomy profile: Hepeviridae. *J Gen Virol* 98:2645–2646.
41. Yin X, et al. (2017) Hepatitis E virus persists in the presence of a type III interferon response. *PLoS Pathog* 13:e1006417.
42. Aye TT, et al. (1992) Complete nucleotide sequence of a hepatitis E virus isolated from the Xinjiang epidemic (1986-1988) of China. *Nucleic Acids Res* 20:3512.
43. Yin X, Ambardekar C, Lu Y, Feng Z (2016) Distinct entry mechanisms for nonenveloped and quasi-enveloped hepatitis E viruses. *J Virol* 90:4232–4242.